Development of Tungsten Repair Technology by Atmospheric Plasma Spraying of Tungsten and Friction Stir Processing

Phuangphaga Daram[1], Yoshiaki Morisada[2], Takuya Ogura[2], Masahiro Kusano[1], JuHyeon Yu[3], Makoto Fukuda[4], Hidetoshi Fujii[2], Seiji Kuroda[1], Makoto Watanabe[1*]

[1] Research Center for Structural Materials, National Institute for Materials Science, Tsukuba, Ibaraki 305-0047 Japan.

[2] Joining and Welding Research Institute, Osaka University, Suita, Osaka 567-0047, Japan.

[3] Rokkasho Institutes for Fusion Energy, National Institutes for Quantum Science and Technology, Kamikita, Aomori 039-3212, Japan.

[4] Naka Institutes for Fusion Science and Technology, National Institutes for Quantum Science and Technology, Naka, Ibaraki 311-0193, Japan.

*Corresponding author: E-mail: watanabe.makoto@nims.go.jp; Tel: +81(0)29-859-2469; Fax:-; Postal address: Research Center for Structural Materials, National Institute for Materials Science, Tsukuba, Ibaraki, 305-0047 Japan.

Abstract

Tungsten (W) has a high melting point, excellent thermal conductivity, and irradiation resistance, making it the most promising plasma facing material for divertors in fusion reactors, which are currently under development. However, since the divertor is exposed to an extremely harsh environment, it is considered necessary to develop suitable and cost-effective repair techniques. In this study, the applicability of the atmospheric plasma spraying (APS) method using a gas shroud as a repair technique for W components was investigated, in particular the

possibility of strengthening the repaired part by applying friction stir processing (FSP) as a post-treatment. It was found that the application of a gas shroud can suppress in-flight oxidation to some extent, even when the W is deposited in air. In addition, the FSP treatment reduced grain size and porosity, resulting in an increase in microhardness of approximately 37.5% compared to the base material (W substrate) and 203.5% compared to the as-sprayed material. The gas shroud APS and FSP post-treatments have been shown to have potential as repair techniques for tungsten components in future fusion reactors.

Keywords: atmospheric plasma spray process; divertor; friction stir processing; microstructure; nuclear fusion reactor; tungsten

Introduction

A nuclear fusion reactor system is a complex arrangement of components designed to facilitate and control nuclear fusion reactions in order to release energy in a controlled and sustainable manner. The International Thermonuclear Experimental Reactor (ITER) is a notable example of a collaborative project aimed at demonstrating the feasibility of nuclear fusion as a large-scale and sustainable energy source (Ref 1). In nuclear fusion reactors, a divertor is a crucial component designed to manage and control the exhaust of particles and heat generated during the fusion process. Its primary purpose is to divert and guide the plasma away from the main chamber of the reactor, thereby protecting the walls and other components from excessive heat and damage (Ref 2, 3). The divertor in a nuclear fusion reactor is crucial due to the extreme conditions in a nuclear fusion reactor, including high temperatures, intense radiation, and exposure to plasma (Ref 2). The divertor is exhaust system in the nuclear fusion reactor to eliminat helium ash and other impurities from the plasma as well as convected heat from the fusion reactors. Tungsten (W) is the primary materials for divertors due to its high melting point,

high thermal conductivity, and good resistance to erosion by plasma particles (Ref 4, 5). It also has low tritium retention, which is advantageous for fuel recycling. Since 2013, the ITER Organization (IO) has recommended high-performance W monoblock technology for divertors. Researchers are actively exploring improvements in design, fabrication techniques, and materials to optimize divertor performance in the demanding environment of fusion reactors (Ref 4-7). However, the surface of the divertor can be damaged due to several factors associated with the extreme conditions of the fusion process, such as thermal loading, plasma surface interactions, and neutron bombardment. (Ref 8). Therefore, processing technologies that enables the simple repair of early-stage wear is crucial for obtaining insights into the operational efficiency and economics of the prototype reactor. The material processing requirements of repair the wall of divertor is focused on dimensional recovery, high-strength bonding between the repaired materials and the base material, high thermal conductivity, etc. Hence, in this study research the development of fundamental technologies enabling the repair of a W surface is the interested research.

Thermal spray techniques provide significant cost savings and durability while reducing working time. An atmospheric plasma spray (APS) process is a thermal spray technique that utilizes a high-temperature plasma to produce a high-quality coating. APS can produce highly adherent coatings on a substrate with a uniform and fine-grained microstructure, imparting exceptional mechanical properties to them (Ref 9). Some relevant works include that by Huang et al. (Ref 10) who, in the context of a design study for W coatings, prepared them on copper (Cu) using a high-speed atmospheric plasma spray (HPAS) technique. The coatings exhibited a good microstructure and relatively low oxygen content. The HAPS technique for depositing W coatings could provide a convenient and low-cost method, making it potentially suitable for

fusion applications. Nevertheless, the microstructures of thermal spray coatings are normally heterogeneous, with unmelted particles, porosity, and oxides weakening mechanical properties. To reduce the defects from thermal spray coating, further post-treatments, such as heat treatment (HT), friction stir processing (FSP), shot peening (SP), and laser remelting (LRM), are essential for sprayed coatings. The HT process is the most widely known process for post-treatment of whole thermal sprayed coatings, which is performed by a heater (furnace) under high temperature, while the FSP is the very strong thermal-mechanical process, and the SP process is the typical mechanical process. The FSP uses the rotating pin tool to form a very fine-grained microstructured surface, and the SP is an excellent modification technique to reduce the cracks in the coating by the peening body, which has the hardest impact on the coating and develops the surface in a plastically deformed condition. Another one by the LRM is a process that utilizes the thermal energy of laser beam to rapidly melt with rapid cooling on the coating, which generate the high-density coating (Ref 11). Wang et al. (Ref 12) studied the effects of annealing under vacuum and a hydrogen atmosphere on the properties of an APS-W coating. The annealing treatment can reduce the tungsten oxides, leading to improvements in thermal conductivity, microhardness and other performance aspects of the APS-W coating. However, vacuum annealing at high temperatures damaged the interface between the APS-W coating and the copper substrate. Furthermore, many investigations of heat treatment techniques using an electrical furnace have shown that this approach may not be sufficient for on-site applications because of limited of the size of repair parts. Similarly, the high energy density of laser by LRM post-treatment could damage the base material, and the oxides possibly result from the oxidation by the material remelting reacted with ambient atmosphere (Ref 11-12). Among these processes, the friction stir processing (FSP) is the one of the mechanical post processing methods with low temperature

used to enhance their properties, improve adhesion, and optimize the performance of thermal spray coatings. This process leads to severe plastic deformation and dynamic recrystallization, resulting in the formation of a very fine-grained microstructural surface (Ref 13-15). FSP provides excellent modification of surface properties along with the removal of defects from the coatings, resulting in advantages in terms of improving the microstructures and properties of coated surfaces (Ref 13). Huang et al. modified cold-sprayed Ni-Ti coatings by comparing two methods: high-temperature vacuum annealing (HTVA) and the FSP processes. Their results showed that applying FSP to an as-sprayed coating can significantly improve the microstructures and mechanical properties. Compared to HTVS, FSP presents a potential method of modifying dense coatings and properties to improve the thermal spray coatings (Ref 16). In the W coatings, Tannigawa et al., improved the thermal conductivity and the hardness values of a vacuum plasma spray (VPS) W coating by the FSP process, resulting in enhance both in mechanical and thermal properties of VPS-W coating on ferritic/martensitic steels (Ref 17). The successful post-treatment process of the the W coating by the FSP process can also significantly reduce the oxide content and porosity along with improve the mechanical properties.It is possible to apply the post-treatment of the W coating in order to modify the microstructure (fine grain, less porosity, low oxide content). This microstructure and property analysis is critical because this understanding will help a specific development to tailor the desired microstructure and parameter process, which apply for the tungsten repair technology in nuclear reactor applications.

Therefore, the objective of this study was to develop fundamental technologies to enable the repair of the W surfaces. This involved combining two processes: (1) atmospheric plasma spray (APS) for material build-up, and (2) friction stir processing (FSP) for strengthening the

build-up section. To clarify technical challenges and optimize each process as a repair technique, actual simulations of tungsten repair were attempted using these processes.

Materials and Methods

Atmospheric plasma spray process conditions

A commercially available 99.9% purity tungsten feedstock powder (D100, manufactured by Allied Materials), with particle diameters in the range of 7-12 μm, was used as feedstock powder, and a tungsten plate (ITER grade for a divertor in a nuclear fusion reactor), with a size of 20x20x3 mm^3 was grit-blasted and ultrasonically cleaned before deposition. The plasma spraying of the W powder was carried out using an APS system (TriplexPro-210, Oerlikon Metco) with a 9 mm internal diameter nozzle and a gun moving speed of 500 mm/s. The coating thickness for all the deposits was maintained at more than 1 mm. To prevent oxidation of powders during spraying, a spray torch with shroud gas was used, as shown in Fig. 1(a). The obtained results were compared with those of the APS without shroud gas. The APS process parameters on each condition are shown in Table 1.

Simulated repair of a divertor by APS process and post-treatment by FSP

Figure 1(b) show a schematic diagram of the simulated step on the divertor. First, the surface of the W plates was damaged by laser irradiation. A 3D printing device (SLM280, SLM Solutions) was used for laser irradiation, with a laser output of 500 W, a scan speed of 300 mm/s, a hatch width of 0.1 mm, and circular scan area with a diameter of 6 mm. The damaged area was then hollowed out by an electrical discharge machine. The removed area was cylindrical, with a diameter of 6 mm and a depth of approximately 0.28 mm measured by optical profilometry, as shown in Fig.2(a). After that, a W overlay was applied to the damaged area using the APS spraying process (Fig. 2(b)), which was selected as the best condition parameter from section 2.1.

Further explanation is provided in section 3. The surface overlay was made flat to some extent by blasting and surface grinding (as shown in after grinding in Fig.2(b)). The FPS was selected for mechanical post-treatment on the repaired W area to optimize the overlay performance. The process was performed using a φ12 mm WC-Co plate tool (a tool without a small protrusion on the tip). The tool was positioned at 0^{o} from the process direction, and a constant tool rotation speed of 500 rpm was maintained. The downward push force was controlled at 0.16 MPa, and the holding time was set to 30 seconds without moving the tool, as shown in the photographs in Fig. 2(c).

Analytical characterization

The cross-sectional microstructure of the samples was obtained using a JSM-6010 scanning electron microscope (SEM: JSM-6010, JEOL) at an accelerating voltage of 20 kV and an electron backscattered diffraction technique (EBSD: JSM-7100F, JEOL), using a step size of 0.3 μm. The oxygen and oxide contents in the coatings were measured using an energy-dispersive X-ray detector (EDS) and an X-ray diffraction system (XRD: Rigaku) with Cu Kα radiation (λ = 1.54060 Å). The XRD data were collected from the range of 2θ = 10-80° with a step size of 0.02°. Vickers hardness measurements were performed using a Matsuzawa AMT-7FS hardness tester with a load of 300gf. The average hardness values and standard deviations were determined.

Results and Discussion

The W coating prepared by APS process.

Figure 3 displays photographs of W coatings prepared using different APS process parameter without a shroud gas, for all thermal sprayed coatings. It can be observed that W coating deposition was successfully using 350 A and Ar = 50 L/min (sample 1). The other samples (samples 2-11) were not sufficient, resulting in local delamination of the coating from

the substrate despite the deposition of a continuous coating. The addition of helium (He) or hydrogen (H_2) with argon (Ar) used in plasma spraying increased both the specific enthalpy and thermal conductivity of the plasma flow, especially at temperatures where dissociation and ionization occurred (Ref 18, 19). Simply increasing the current together with the gas mixture in plasma spraying during in situ structuring resulted in coating delamination during deposition (Ref 19). It is assumed that the increased heat input into the substrate and higher tensile stresses caused this delamination. Based on the overall morphology after deposition, the parameters used for sample 1 are selected to build a W coating for repairing the divertor in a nuclear fusion reactor.

After the APS parameters were selected, a shroud gas was used in the APS process to reduce oxidation during spraying. Figure 4(a) shows photographs of W coatings produced using different spraying distances of the shroud gas. The results showed that all coatings deposited the W feedstock powders onto the W plate continuously, achieving a thickness of 1-1.5 mm (Fig. 4(b)). The coatings prepared by APS with a shroud gas were expected to have a dense lamellar microstructure with low oxide contents. The backscattered electron (BSE) image in Fig. 4(b) also reveals that a dense cross-section at a low level of porosity and an oxide layer in the shrouded W coating (sample 16) was achieved; only a few gray areas indicate the presence of oxide layers. The high shielding gas flow rate can prevent the agglomerated oxidized features from being swept away by the gas, effectively flushing away fine dust and oxidized splash droplets during deposition (Ref 20). This is impact on achieving the lowest oxide contents in the shrouded W coating under the processing parameter conditions used for sample 16. A comparison of oxygen contents on the W coatings is shown in Fig. 5. The results showed that the oxygen contents of the W coating sprayed at less than 120 mm (sample 15) and 140 mm (sample 16) of distance were

~0.62 and ~0.59 wt.%, respectively. The oxygen contents of the shrouded W coatings are 25% lower than that of the unshrouded coating (sample 1). Similar to the oxygen content results by the EDS, the characteristic peaks for WO_3 and WO_2 can be found in the XRD patterns from all W coatings with/without shrouded gun, which is the possible oxide phases in the thermal sprayed W coating (Fig. 6). The XRD pattern of the sample 15, 16 and 1(unshrouded) exhibited lower intensity WO_3 and WO_2 peaks than the other samples. When the diffraction angle from 23 to 25° of the WO_3 phase was enlarged, it was confirmed that the oxide content in sample 16 was lower than that of sample 15 and 1. Clearly, the APS equipped with shrouded gun can reduce the oxidation during in-fight spraying process. The shroud system in the APS process is designed to create an oxygen-reduced or inert atmosphere, and an atmospheric plasma gun is attached to its end. This minimizes the risk of oxidation during the spraying process, which is critical for a W coating (Ref 21). The spray distance is close to the substrate, it may be affected by the plasma. The temperature of the substrate to rise too high, and it would be heavily oxidized due to the influence of the flame flow and thermal deformation. Therefore, the oxide contents of sample 14 (100 mm) was higher than that of sample 15 (120 mm) and 16 (140 mm), respectively. Moreover, the high shielding gas flow rate (157 L/min for samples 15 and 16) displaces the ambient air in the spraying environment to create a barrier that prevents direct contact between the W powder and oxygen from the ambient air, results in lower coating oxide contents compared to the low shielding gas flow rates (17 L/min (sample 12) and 85 (sample 13). These results are similar to what has been achieved with inert gas shrouding in a hybrid water argon plasma spraying of W and Cu coatings (Ref 22). The inert gas shrouding, tightly attached to the torch front, was found to effectively reduce the extent of in-flight oxidation, especially when a reduced outlet orifice was used (Ref 20, 23).

The W overlay before and after the FSP treatment to repair a divertor on a nuclear fusion reactor

BSE and IPF images in Fig. 7 show the microstructure of the simulated cross-sectional damaged area on the surface of W plate after applying the laser radiation. The results present that vertical crack with a depth of 200-500 μm due to thermal and mechanical stresses during high power laser beam by SLM across the W surface. Moreover, additional heating/remelting from laser radiation caused by the grain microstructure, resulting in the grain size in damaged area is larger than that of the W plate because of remelting by laser radiation. Moreover, the microstructure of damaged area shows the columnar grains that grew epitaxially on the previously solidified track similar to the normally microstructure of SLM samples (Ref. 24). This is area was removed by electrical discharged before deposit the APS-W overlay and FSP process in order to simulate the repair the wall of the W divertor. Fig. 8 shows the microstructures of the W overlays before and after FSP treatment to fill up the damaged area on the surface of the W plate, giving an overview and details of the W overlay structure. There are some pores and oxide layers in the W overlay. The W overlay after the FSP treatment (Fig. 8(b)) appears to have a denser and finer microstructure compared to the W overlay before the FSP treatment (Fig. 8(a)). Before the FSP treatment, the overlay mainly exhibited a lamellae structure, splat boundaries, oxide layers (gray color), and pores (black color). In addition, the W grain in the lamellae structure formed a columnar structure, as seen in an inverse pole figure (IPF) image (Fig. 8(a)) by EBSD analysis. The orientation of this overlay is random because the thermal energy was inadequate to form the preferred orientation during rapid cooling by the APS process (Ref. 25). The kernel average misorientation (KAM) map before the FSP treatment appears mostly blue, indicating a general assumption of low plastic deformation in the W overlay prepared by the APS process. After the

FSP treatment (Fig. 8(b)), the microstructure of the W overlay underwent significant changes, resulting in an extremely dense with low porosities near surface. As the IPF image reveals, there is a significant presence of a recrystallized and fine equiaxed grain structure, which is smaller in term of grain size compared to those observed in the W overlay before FSP treatment. A large number of ultrafine grains were observed in the FSP region near the surface. During the FSP treatment, the W overlay undergoes severe plastic deformation by non-equilibrium grain boundaries with high energy and long-range stresses caused by the absorption of a large number of lattice dislocations. Furthermore, the KAM map predominantly displays green and blue colors, indicating increased local dislocation density and the formation of dislocation pileup after the FSP treatment. Therefore, it appears that this could be due to grain boundary sliding or other boundary-dominated strain accommodation mechanisms (Ref 14-16). The FSP treatment refined the microstructure, resulting in the appearance of fine and equiaxed grains at near the surface, specifically in the stir zone. This transformation is influenced by maximum strain, peak temperature and the occurrence of dynamic recrystallization (Ref 15-17, 26, 27). During FSP, the intense plastic deformation and frictional heating generated by the rotating tool can create elevated temperatures in the material (Ref 26). The W overlay undergoes varying combinations of strain and temperature within the stir zone, leading to non-uniform plastic deformation or a strain gradient. However, the grain size near the surface appears finer than that in the lower area near the bottom indicating the presence of a possible strain gradient. This variation can be attributed to the different degree of deformation and temperature experienced in these areas due to variations in material flow patterns around the tool. The area near the bottom overlay (lower zone) involves relatively lower strains and temperatures compared to the area near the surface (upper zone), which belong to the thermomechanically affected zone (Ref 26). This area

undergoes slight recrystallization due to insufficient strain and a high rate of dynamic recovery, leaving the grain structure little changed. Compared to other treatments on W coatings (Ref 12, 25), the FSP treatment showed a refined microstructure with decreased oxide and porosity, while post-treatment by a vacuum annealing and a press annealing on the W coatings reported by Park et al. (Ref 25) showed no obvious differences in microstructure and slightly decreased the influences of some defects, such as oxides and splat boundary problems. In addition, the annealing process also causes a certain damage to the tungsten copper interface, especially as a result of vacuum annealing at a high temperature, as reported by Wang, et.al. (Ref 11).

The average hardness values of the W overlay before and after the FSP treatment compared to the W plate are shown in Fig. 9(a). It can be observed that the hardness values of the W plate on slightly decreased when applying laser radiation. This causes increases in the grain size and the vertical crack results in a reduction in the hardness of them. For the hardness value of the W overlay before the FSP treatment was about 202±30 HV, which is lower than that of the overlay after the FSP treatment (613±104 HV). Moreover, the hardness value of the overlays after the FSP increased by about 1.3-1.5 times compared to that of the W plate (446±21 HV). As previously explained regarding the microstructure of the W overlay after the FSP treatment, it is evident that the FSP, as a surface reinforcement method, is effective in developing grain refinement in the W overlay. The grain refinement formed as a result of dynamic recrystallization, along with the reduced porosity, is responsible for the increase in hardness at the FSP area. The schematic diagram of changing hardness before and after applied the FSP compared to the W base materials is shown in Fig. 9(b). Similar to the other works (Ref 14-16, 28), especially the VPS-W by moving tip single and double pass of the FSP, reported by Tanigawa et al. (Ref 17), demonstrated the refinement of grain structure and reduction in porosity in thermal sprayed

coatings through the FSP treatment, contributing to increased hardness and improved wear resistance. It can assume that both FSP without moving tip of this work and with moving tip of Tanigawa et al. (Ref 17) can modify and improve the microstructure and mechanical properties of the W coating. However, a heat input of the FSP without moving tip can modify the deeper section near the W plate, which indicate in the hardness values of the lower area of FSP area (573±116 HV) that slightly lower than that of the upper area but still higher than that of the W plate. According to the well known Hall-Petch equation (Ref 29, 30), the changes in yield stress (and hence the hardness) are inversely proportional to variations in the square root of grains size, and the high density of dislocation formed by the FSP. Therefore, the smaller the grain size, the higher the hardness will be, as demonstrated near the surface. Moreover, the high dislocation density and sub-grain boundaries also contribute to an improvement in strength, as they act as obstacles for dislocation motion (Ref 29, 30). The low oxide content, dense and high hardness values of the W overlay produced using the APS process with the FSP treatment, have the potential to repair and protect the surface of a W divertor in a nuclear fusion reactor from thermal stress, plasma surface interactions, and neutron bombardment. This material can be considered suitable for use under these work conditions.

Conclusions

The development of a repair technology for tungsten parts that can be applied to a divertor on a nuclear fusion reactor led to the following results.

This work optimized the parameter conditions for depositing a W coating by the APS process. Additionally, the use of a shroud gas has achieved certain results in suppressing oxidation in the coating, reducing the oxygen content by 25%. Furthermore, it was easily possible to obtain a thick coating of 1 mm or more on the W substrate.

Successful repair in the damaged area were achieved by simulating repair on the W plate using the APS and the FSP treatment processes, with the application of a W overlay prepared through both of these processes. The results demonstrate that the W overlay, after the FSP treatment, can effectively enhance the performance of the W overlay produced by the APS process. This enhancement includes reducing grain size, and porosity of the overlay. As a result, the hardness of the repaired part increased by 1.3 to 1.4 times that of the base metal.

The APS and the FSP treatment processes can be combined to repair the surface of the divertor part, resulting in the W overlay with fine structure, dense and low oxides content, which enhances its properties and performance, including mechanical properties. It can be expected that APS-W with FSP can become the candidate process the development of tungsten repair technology. This maintenance concepts hold the potential to ensure an acceptable level of applicability to future fusion power reactors. Nevertheless, the microhardness result is not enough to explain the properties for the future fusion power reactor applications. Considering the practical application, future work is necessary to systematically unravel the mechanical and other properties, such as tensile properties, wear resistance, erosion resistance, and radiation effects, etc.

Acknowledgment

This work is performed with the support and under the auspices of the NIFS Collaboration Research program (NIFS21HDAF007).

References

1. P.-H. Rebut, ITER: The First Experimental Fusion Reactor, *Fusion. Eng. Des.,* 1995, **30**(1-2), p 85-118. https://doi.org/10.1016/0920-3796(94)00403-T
2. Divertor. https://www.iter.org/mach/Divertor, 2023. Accessed 26 Dec 2023.

3. I. Palermo, R. Villari and A. Ibarra, Divertor Options Impact on DEMO Nuclear Performances, *Fusion. Eng. Des.*, 2018, **130,** p 32-41. https://doi.org/10.1016/j.fusengdes.2018.03.020

4. Y. Huang, M.S. Tillack and N.M. Ghoniem, Tungsten Monoblock Concepts for the Fusion Nuclear Science Facility (FNSF) First Wall and Divertor, *Fusion. Eng. Des.*, 2018, **135**, p 346-355. https://doi.org/10.1016/j.fusengdes.2017.06.026

5. T. Fu, K.Cui, Y. Zhang, J. Wang, F. Shen, L. Yu, J. Qie and X. Zhang, Oxidation Protection of Tungsten Alloys for Nuclear Fusion Applications: A Comprehensive Review, *J. Alloys. Compd.*, 2021, **884**, p 161057. https://doi.org/10.1016/j.jallcom.2021.161057

6. T. Hirai, S. Panayotis, V. Barabash, C. Amzallag, F. Escourbiac, A. Durocher, M. Merola, J. Linke, Th. Loewenhoff, G. Pintsuk, M. Wirtz and I. Uytdenhouwen, Use of Tungsten Material for the ITER Divertor, *Nucl. Mater. Energy.,* 2016, **9**, p 616-622. https://doi.org/10.1016/j.nme.2016.07.003

7. K. Ezato, S. Suzuki, Y. Seki, T. Hirayama, H. Yamada, F. Escourbiac and T. Hirai, Development of Tungsten Divertor Components for ITER in Japan, *Fusion Eng. Des.,* 2018, **136**, p 683-689. https://doi.org/10.1016/j.fusengdes.2018.03.057

8. H. Bolt, V. Barabash, G. Federici, J. Linke, A. Loarte, J. Roth and K. Sato, Plasma Facing and High Heat Flux Materials-Needs for ITER and Beyond, *J. Nucl. Mater.*, 2002, **307-311**, p 43-52. https://doi.org/10.1016/S0022-3115(02)01175-3

9. S.-H. Liu, J.P. Trelles, C.-J. Li, C.-X. Li and H.-B. Guo, A Review and Progress of Multiphase Flows in Atmospheric and Low Pressure Plasma Spray Advanced Coating, *Mater. Today Phys.,* 2022, **27,** p 100832. https://doi.org/10.1016/j.mtphys.2022.100832

10. J. Huang, F. Wang, Y. Liu, S. Jiang, X. Wang, B. Qi and L. Gao, Properties of Tungsten Coating Deposited onto Copper by High-Speed Atmospheric Plasma Spraying, *J. Nucl. Mater.,* 2011, **414**(1), p 8-11. https://doi.org/10.1016/j.jnucmat.2011.04.019

11. W. Sun, A.W. Tan, K. Wu, S. Yin, X. Yang, I. Marinescu and E. Liu, Post-process Treatments on Supersonic Cold Sprayed Coatings: A Review, *Coatings.* 2020, **10**, p 123. https://dx.doi.org/10.3390/coatings10020123

12. F. Wang, G.-N. Luo, J. Huang and Y. Liu, Properties Improvement of Atmospheric Plasma Sprayed Tungsten Coating by Annealing, *Surf. Coat. Technol.,* 2019, **358,** p 276-281. https://doi.org/10.1016/j.surfcoat.2018.11.046
13. R.S. Mishra and Z.Y. Ma, Friction Stir Welding and Processing, *Mater. Sci. Eng., R,* 2005, **50**(1-2), p 1-78. https://doi.org/10.1016/j.mser.2005.07.001
14. W. Wang, P. Han, P. Peng, T. Zang, Q. Liu, S.-N. Yuan, L.-Y. Huang, H.-L. Yu, K. Qiao and K.-S. Wang, Friction Stir Processing of Magnesium Alloys: A Review, *Acta Metall. Sin. (Engl. Lett).,* 2020, **33,** p 43-57. https://doi.org/10.1007/s40195-019-00971-7
15. Y. Morisada, H. Fujii, T. Mizuno, G. Abe, T. Nagaoka and M. Fukusumi, Modification of Thermally Sprayed Cemented Carbide Layer by Friction Stir Processing, *Surf. Coat. Technol.,* 2010, **204**(15), p 2459-2464. https://doi.org/10.1016/j.surfcoat.2010.01.021
16. C.J. Huang, X.C. Yan, W.Y. Li, W.B. Wang, C. Verdy, M.P. Planche, H.L. Liao and G. Montavon, Post-Spray Modification of Cold-Sprayed Ni-Ti Coatings by High-Temperature Vacuum Annealing and Friction Stir Processing, *Appl. Surf. Sci.*, 2018, **451,** p 56-66. https://doi.org/10.1016/j.apsusc.2018.04.257
17. H. Tanigawa, K. Ozawa, Y. Morisada, S. Noh and H. Fujii, Modification of Vacuum Plasma Sprayed Tungsten Coating on Reduced Activation Ferritic/Martensitic Steels by Friction Stir Processing, *Fusion. Eng. Des.,* 2015, **98-99**, p 2080-2084. https://doi.org/10.1016/j.fusengdes.2015.04.059
18. R. Djebali, B. Pateyron and M. ElGanaoui, Scrutiny of Plasma Spraying Complexities with Case Study on the Optimized Conditions toward Coating Process Control, *Case Stud. Therm. Eng.,* 2015, **6,** p 171-181. https://doi.org/10.1016/j.csite.2015.09.005
19. A.B. Murphy, Thermal Plasmas in Gas Mixtures, *J. Phys. D: Appl. Phys*., 2001, **34,** p R151-R173. https://doi.org/10.1088/0022-3727/34/20/201
20. S. Matthews, Shrouded Plasma Spray of Ni-20Cr Coatings Utilizing Internal Shroud Film Cooling, *Surf. Coat. Technol.,* 2014, **249**, p 56-74. https://doi.org/10.1016/j.surfcoat.2014.03.050

21. D. Hu, X. Zheng, Y. Niu, H. Ji, F. Chong and J. Chen, Effect of Oxidation Behavior on the Mechanical and Thermal Properties of Plasma Sprayed Tungsten Coatings, *J. Therm. Spray. Tech.,* 2008, **17**, p 377-384. https://doi.org/10.1007/s11666-008-9190-4

22. J. Matějíček, T. Kavka, G. Bertolissi, P. Ctibor, M. Vilémová, R. Mušálek and B. Nevrlá, The Role of Spraying Parameters and Inert Gas Shrouding in Hybrid Water-Argon Plasma Spraying of Tungsten and Copper for Nuclear Fusion Applications, *J. Therm. Spray. Tech.,* 2013, **22,** p 744-755. https://doi.org/10.1007/s11666-013-9895-x

23. M. Jankovic, J. Mostaghimi and V. Pershin, Design of a New Nozzle for Direct Current Plasma Guns with Improved Spraying Parameters, *J. Therm. Spray. Tech.,* 2000, **9,** p 114-120. https://doi.org/10.1361/105996300770350140

24. W. E. Frazier, Metal Additive Manufacturing: A Review, *J. Mater. Eng. Perform.,* 2014, **23**, p 1917-1928. https://doi.org/10.1007/s11665-014-0958-z

25. J.Y. Park, S.J. Yang, Y.G. Jin, C.R. Park, G.H. Kim and H. N. Han, Effect of Annealing with Pressure on Tungsten Film Properties Fabricated by Atmospheric Plasma Spray, *Met. Mater. Int*., 2014, **20**, p 1037-1042. https://doi.org/10.1007/s12540-014-6006-6

26. D. Yadav and R. Bauri, Effect of Friction Stir Processing on the Microstructure and Mechanical Properties of Aluminum, *Mater. Sci. Eng. A.,* 2012, **539,** p 85-92. https://doi.org/10.1016/j.msea.2012.01.055

27. G. Huang, J. Wu, W. Hou and Y. Shen, Microstructure, Mechanical Properties and Strengthening Mechanism of Titanium Particle Reinforced Aluminum Matrix Composites Produced by Submerged Friction Stir Processing, *Mater. Sci. Eng. A.,* 2018, **734**, p 353-363. https://doi.org/10.1016/j.msea.2018.08.015

28. A. Rahbar-kelishami, A. Abdollah-zadeh, M.M. Hadavi, A. Banerji, A. Alpas and A.P. Gerlich, Effects of Friction Stir Processing on Wear Properties of WC-12%Co Sprayed on 52100 steel, *Mater. Design.,* 2015, **86**, p 98-104. https://doi.org/10.1016/j.matdes.2015.06.132

29. E.O. Hall, The Deformation and Ageing of Mild Steel: III Discussion of Results, *Proc. Phys. Soc. B.*, 1951, **64**, p 747-753. https://doi.org/10.1088/0370-1301/64/9/303

30. N.J. Petch, The Cleavage Strength of Polycrystals, *J. Iron. Steel. Inst.,* 1953, **174,** p 25-28.

Table 1 Parameters for W spraying on an W substrate (ITER grade) by APS

Sample no.		Current, A	Gas types	Gas flow rate, L/min	Spraying distance, mm	Shielding gas flow rate, L/min
Without shroud gas	1	350	Ar	50	100	…
	2	400	Ar	50	100	…
	3	450	Ar	50	100	…
	4	500	Ar	50	100	…
	5	540	Ar	50	100	…
	6	350	Ar/He	50/10	100	…
	7	400	Ar/He	50/10	100	…
	8	450	Ar/He	50/10	100	…
	9	350	Ar/H_2	44/6	100	…
	10	350	Ar/H_2	44/6	100	…
	11	350	Ar/H_2	44/6	100	…
With shroud gas	12	350	Ar	50	100	17
	13	350	Ar	50	100	85
	14	350	Ar	50	100	157
	15	350	Ar	50	120	157
	16	350	Ar	50	140	157

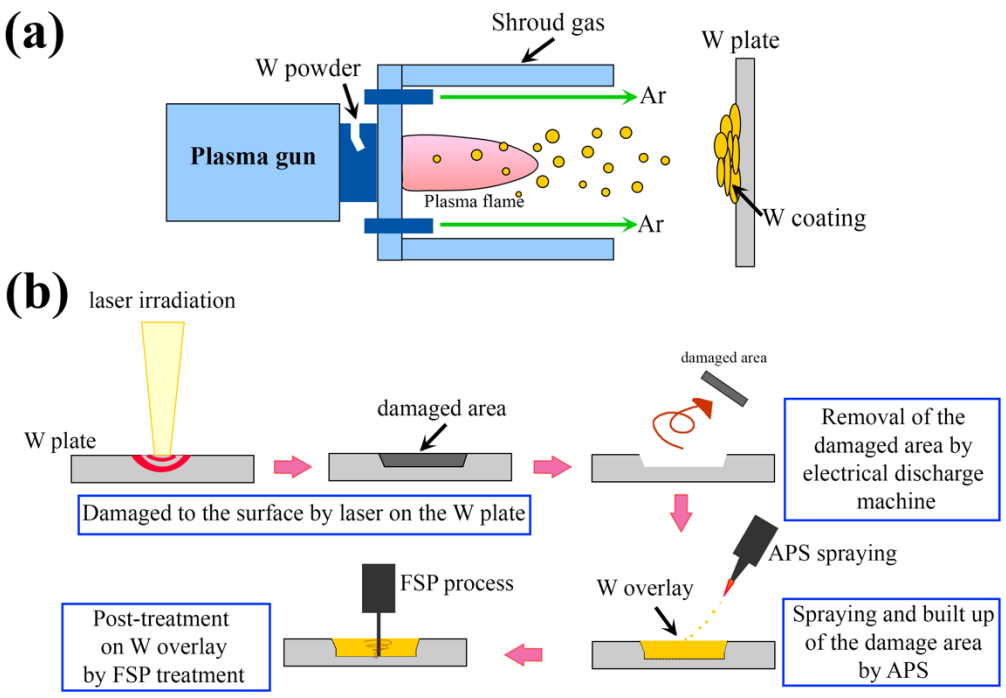

Fig. 1 Schematic diagram of (a) the atmospheric plasma spray (APS) system equipped with the shroud gas and (b) simulated repair of the divertor by the APS process and post-treatment by the friction stir processing (FSP) treatment.

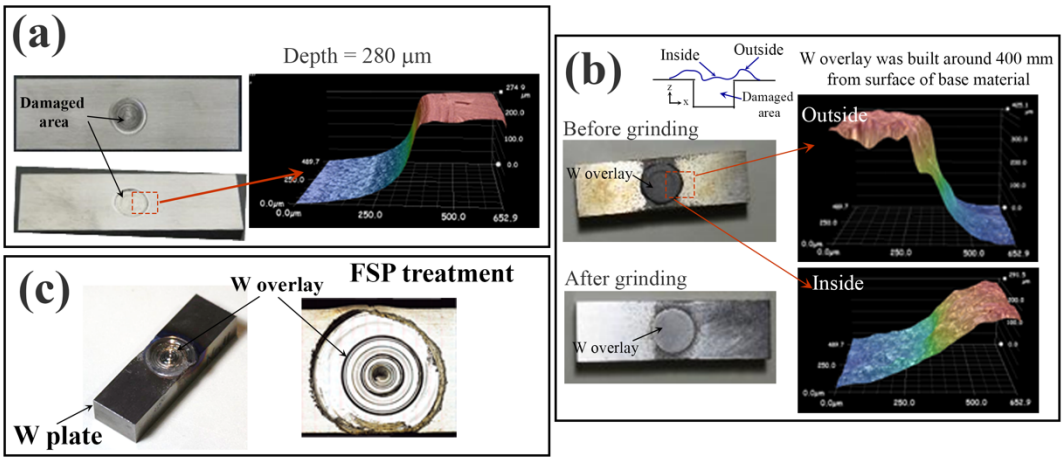

Fig. 2 Photographs and optical profilometry images of simulated repair of the divertor including (a) the damaged area after laser radiation and electrical discharge, (b) the W overlay to fill up the damaged area, and (c) the W overlay after the FSP treatment

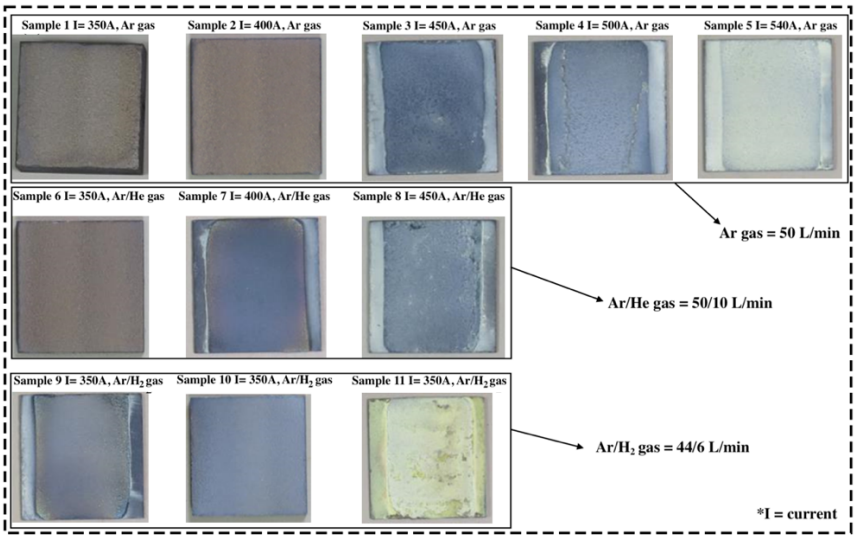

Fig. 3 Photographs of the W coating produced using different process parameters of the APS process without the shroud gas

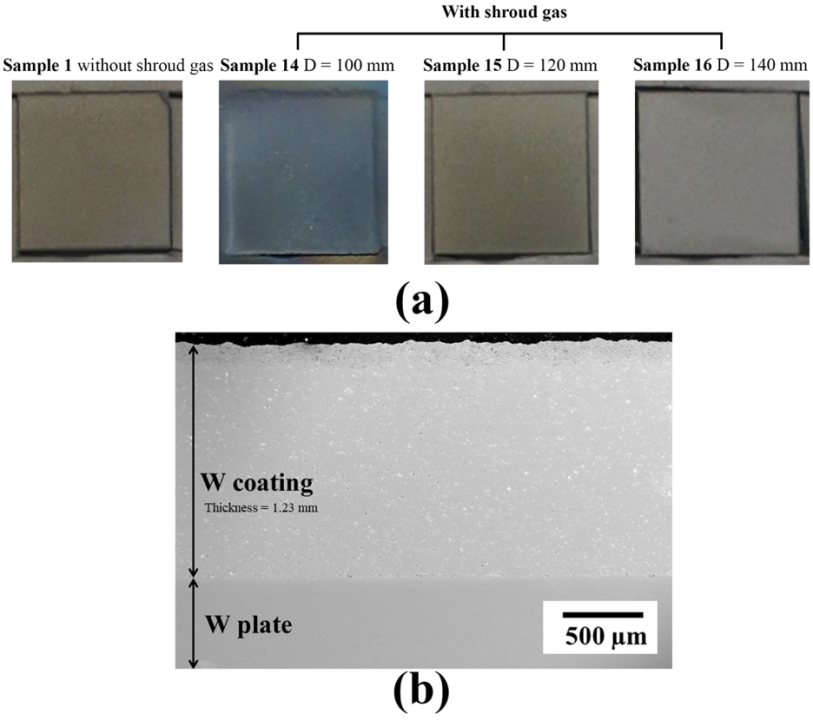

Fig. 4 (a) photographs of the W coating produced using different spraying distances of the APS process with the shroud gas and (b) BSE micrograph of a W coating (sample 16) prepared by the APS process with the shroud gas

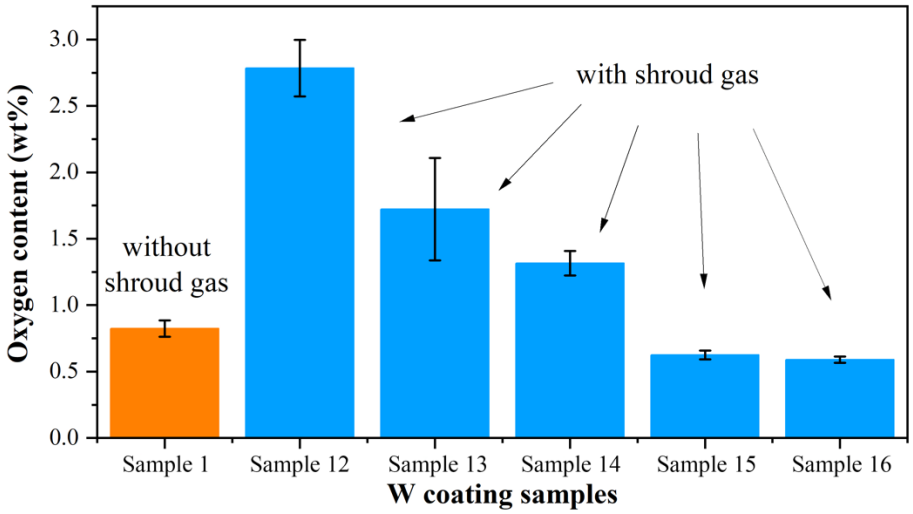

Fig. 5 Oxygen contents of the W coatings prepared by the APS process with or without the shroud gas

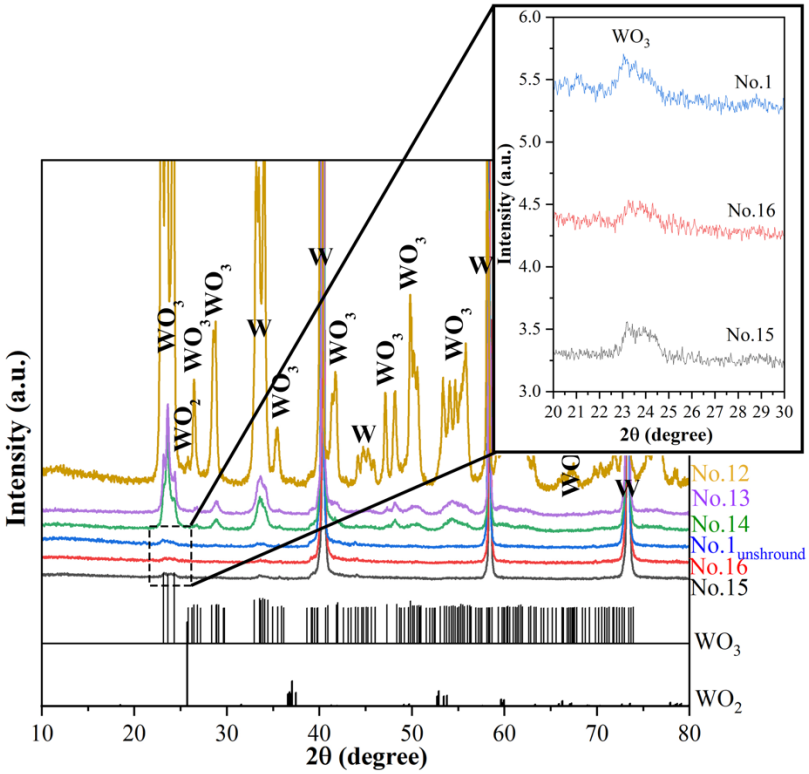

Fig. 6 XRD patterns of the W coatings prepared by the APS process with or without the shroud gas

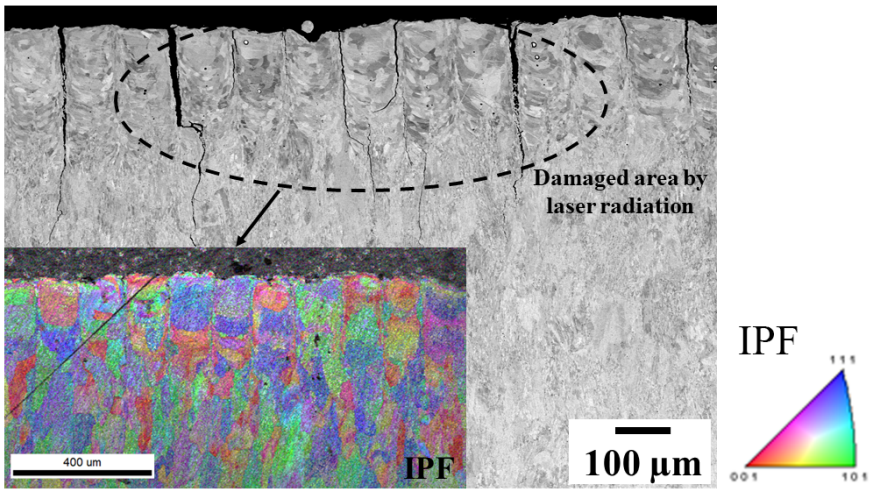

Fig. 7 BSE and IPF images of the microstructure the damaged area on the W plate after applying laser radiation

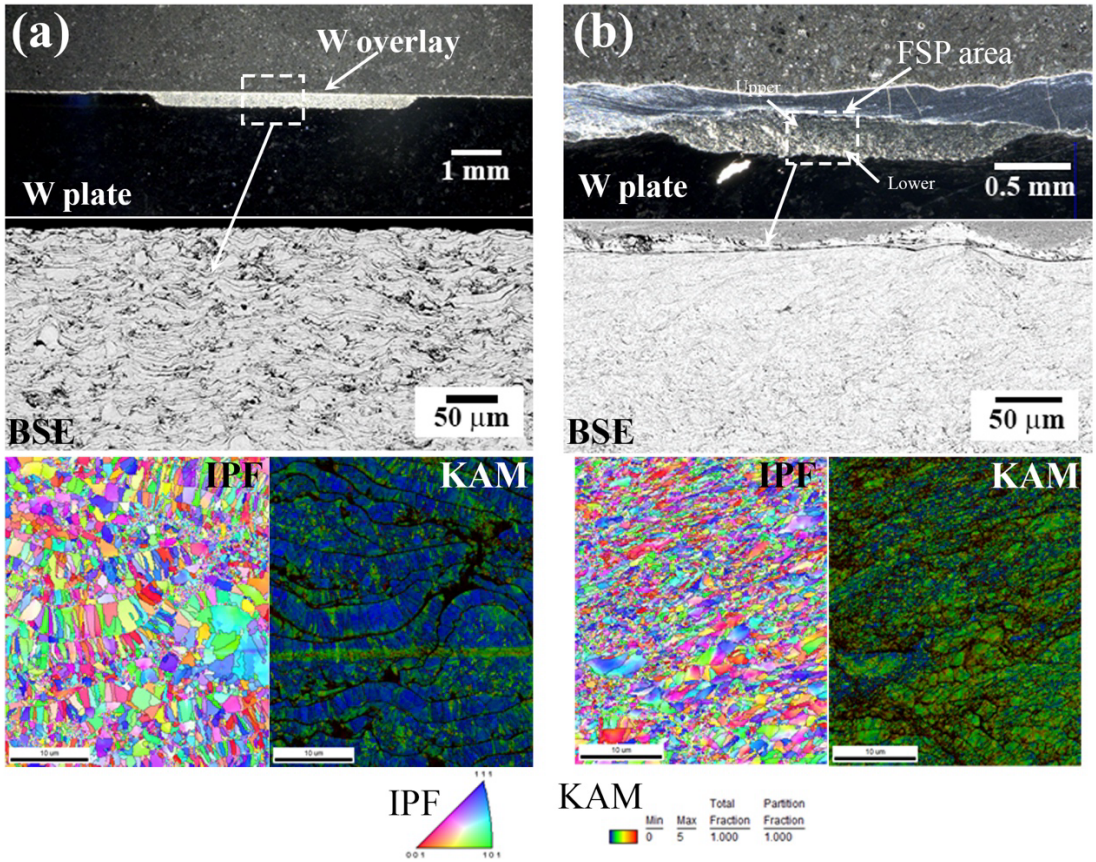

Fig. 8 BSE micrographs, inverse pole figures (IPF), and kernel average misorientations (KAM) of the cross-sectional W overlays before (a) and after (b) the FSP process

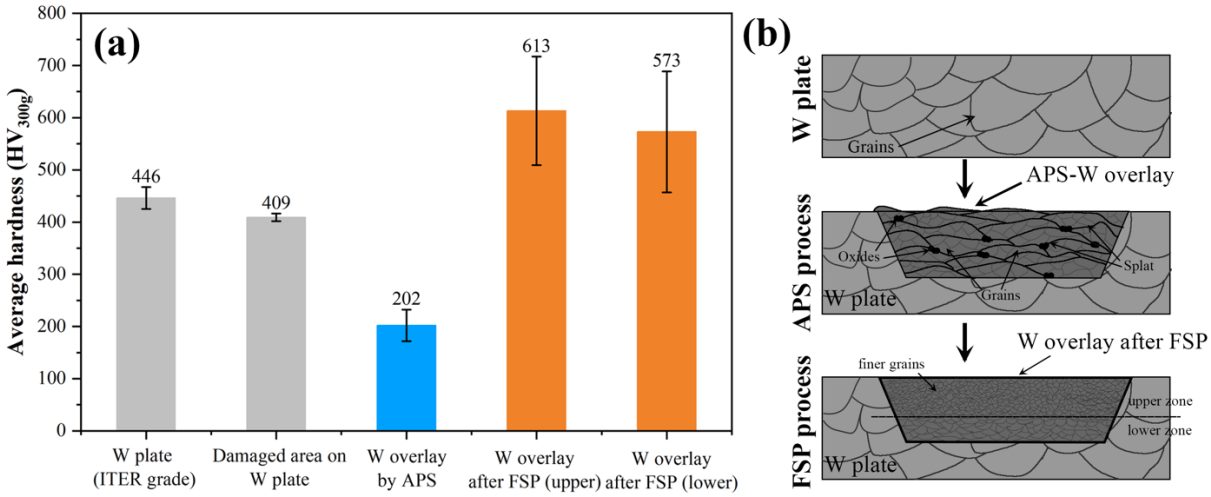

Fig. 9 (a) comparation of average hardness in the W overlays before and after the FSP process and (b) schematic diagram of hardness measurement positions on the specimen